Osmium−Antimony Higher Nuclearity Clusters

Weng Kee Leong* and Guizhu Chen

Department of Chemistry, National University of Singapore, Kent Ridge, Singapore 119260

Received January 19, 2001

Thermolysis of $Os_3(CO)_{11}(SbPh_3)$, **1**, in refluxing octane gave initially the clusters $Os_3(\mu\text{-}SbPh_2)(\mu\text{-}H)(\mu_3,\eta^2\text{-}C_6H_4)(CO)_9$, **2**, and $Os_6(\mu_3\text{-}SbPh)(\mu_3,\eta^2\text{-}C_6H_4)(CO)_{20}$, **3**. Prolonged heating gave the cluster $Os_6(\mu_4\text{-}Sb)(\mu\text{-}H)(\mu_3,\eta^4\text{-}C_{12}H_8)(\mu_3,\eta^2\text{-}C_6H_4)(CO)_{16}$, **4**, as the major product. In contrast, thermolysis in hexane at 115 °C in a Carius tube gave $Os_6(\mu_4\text{-}Sb)(\mu\text{-}SbPh_2)(\mu\text{-}H)_2(\mu_3,\eta^4\text{-}C_{12}H_8)(\mu_3,\eta^2\text{-}C_6H_4)(CO)_{15}$, **5**, $Os_6(\mu_4\text{-}Sb)(\mu\text{-}SbPh_2)(\mu\text{-}H)(\mu_3,\eta^2\text{-}C_6H_4)_2(C_6H_5)(CO)_{16}$, **6**, and $Os_6(\mu_4\text{-}Sb)(\mu\text{-}SbPh_2)(\mu\text{-}H)(\mu_3,\eta^6\text{-}C_6H_4)(\mu_3,\eta^2\text{-}C_6H_4)(C_6H_5)(CO)_{15}$, **7**, besides **2** and **3**. It has been demonstrated that cluster **6** was formed from **2**, while clusters **5** and **7** were formed from the further decomposition of **6**. The reaction of 5 with $SbPh_3$ afforded a monosubstituted derivative, $Os_6(\mu_4\text{-}Sb)(\mu\text{-}H)_2(\mu\text{-}SbPh_2)(\mu_3,\eta^2\text{-}C_6H_4)(\mu_3,\eta^4\text{-}C_{12}H_8)(CO)_{14}(SbPh_3)$, **8**. The clusters **2**−**8** were all shown by single-crystal X-ray crystallographic studies to have a benzyne moiety acting as a four-electron donor to a triosmium fragment. In addition, **4** and **8** contain a novel μ_3,η^4-biphenylene moiety bound to a triosmium framework, while **7** was found to have a $\mu_3,\eta^1{:}\eta^1{:}\eta^6\text{-}C_6H_4$ ring.

Introduction

Despite the increasing trend toward rational synthesis, much of the discoveries in higher nuclearity carbonyl clusters are still based on pyrolytic and redox condensation reactions. Careful control of pyrolytic conditions can lead to useful stepwise decarbonylation as, for example, in the vacuum pyrolysis of $Os_3(CO)_{12}$, which afforded a large number of clusters ranging in nuclearity from 5 to 11,[1] but the conditions can be optimized to give $Os_6(CO)_{18}$ in up to 80% yield.[2] Heteroatoms of the main group can also play an important role in cluster formation. The main group elements may be incorporated into the pyrolysis products via the splitting of organic ligands as, for example, in the thermolysis of $Os_3(\mu\text{-}SR)(\mu\text{-}H)(CO)_{10}$ ($R = CH_2C_6H_5$) to give two isomers of $Os_6(\mu_4\text{-}S)(\mu_3\text{-}S)(\mu\text{-}H)_2(CO)_{17}$ through homolysis of the C−S bond and formation of dibenzyl.[3,4] The condensation of $Os_3(CO)_{10}(NCCH_3)_2$ with $Os_3(\mu_3\text{-}S)_2(CO)_9$ or $Os_4(\mu_3\text{-}S)(CO)_{12}$ gave $Os_6(\mu_4\text{-}S)(\mu_3\text{-}S)(CO)_{17}$ or $Os_7(\mu_4\text{-}S)(CO)_{19}$, respectively,[5] and it is believed that the sulfur atoms played a key role in linking the low-nuclearity cluster units and directing the formation of the new clusters.[6]

Among osmium clusters containing group 15 elements, the classic reaction is that of $Os_3(CO)_{12}$ with excess PPh_3 in refluxing xylene to give a mixture of nine compounds: the substitution derivatives $Os_3(CO)_{12-n}(PPh_3)_n$ ($n = 1-3$); three hydride-bridged species $Os_3(\mu\text{-}PPh_2C_6H_4)(\mu\text{-}H)(CO)_8(PPh_3)$, $Os_3(PPh_2C_6H_4)(\mu\text{-}H)(CO)_9(PPh_3)$, and $Os_3(\mu\text{-}PPh_2)(\mu\text{-}H)(\mu_3,\eta^2\text{-}C_6H_4)(CO)_7(PPh_3)$; and three complexes obtained from loss of phenyl rings, viz., $Os_3(\mu\text{-}PPh_2)(\mu\text{-}PPhC_6H_4)(Ph)(CO)_8$, $Os_3(\mu\text{-}PPh_2)_2(\mu_3,\eta^2\text{-}C_6H_4)(CO)_7$, and $Os_3(\mu\text{-}PPh_2)(CO)_8(PPh_3)$ (Scheme 1).[7] Later work on this reaction and related systems by Deeming's group has led to clarification of much of the reaction pathway; he has demonstrated that the clusters resulting from loss of phenyls and/or orthometalation were formed from thermal decomposition of the substituted products, and it was clear that the nature of the ligand was important in determining the product distribution.[8,9]

In all these thermal decomposition reactions, there were no reports of cluster aggregation to form higher nuclearity clusters. In fact, low yields of dimeric species such as $Os_2(\mu\text{-}AsMe)_2(\mu,\eta^2\text{-}C_6H_4)(CO)_6$ were obtained from the $AsMe_2Ph$ complexes, indicating cluster fragmentation.[8] We have also recently reported that the thermolysis of $Os_3(CO)_{11}(AsPh_3)$ gave rise to four major products, which contained Os_3As or Os_3As_2 cores.[10] Our past experience with antimony-containing clusters has been that they can behave very differently from the phosphine and arsine analogues.[11] We were therefore interested to determine if thermolysis of antimony-containing derivatives of osmium would afford structur-

(1) Braga, D.; Henrick, K.; Johnson, B. F. G.; Lewis, J.; McPartlin, M.; Nelson, W. J. H.; Sironi, A.; Vargas, M. D. *J. Chem. Soc., Chem. Commun*. **1983**, 1132.
(2) Eady, C. R.; Johnson, B. F. G.; Lewis, J. *J. Chem. Soc., Dalton Trans*. **1975**, 2606.
(3) Adams, R. D.; Horvath, I. T.; Segmuller, B. E.; Yang, L. W. *Organometallics* **1983**, *2*, 1301.
(4) Adams, R. D.; Yang, L. W. *J. Am. Chem. Soc.* **1982**, *104*, 4115.
(5) Adams, R. D.; Horvath, I. T.; Yang, L. W. *J. Am. Chem. Soc.* **1983**, *105*, 1533.
(6) Adams, R. D.; Foust, D. F.; Mathur, P. *Organometallics* **1983**, *2*, 990.
(7) (a) Bradford, C. W.; Nyholm, R. S. *J. Chem. Soc., Dalton Trans.* **1973**, *5*, 529. (b) Gainsford, G. J.; Guss, J. M.; Ireland, P. R.; Mason, R.; Bradford, C. W.; Nyholm, R. S. *J. Organomet. Chem*. **1972**, *40*, C70. (c) Bradford, C. W.; Nyholm, R. S.; Gainsford, G. J.; Guss, J. M.; Ireland, P. R.; Mason, R. *J. Chem. Soc., Chem. Commun*. **1972**, 87.
(8) (a) Arce, A. J.; Deeming, A. J. *J. Chem., Soc., Dalton Trans*. **1982**, 1155. (b) Deeming, A. J.; Kimber, R. E.; Underhill, M. *J. Chem., Soc., Dalton Trans*. **1973**, 2589.
(9) (a) Deeming, A. J.; Kabir, S. E.; Powell, N. I.; Bates, P. A.; Hursthouse, M. B. *J. Chem. Soc., Dalton Trans*. **1987**, 1529. (b) Brown, S. C.; Evans, J.; Smart, L. E. *J. Chem. Soc., Chem. Commun*. **1980**, 1021. (c) Deeming, A. J.; Marshall, J. E.; Nuel, D.; O'Brien, G.; Powell, N. I. *J. Organomet. Chem*. **1990**, *384*, 347.
(10) Tay, C. T.; Leong, W. K. *J. Organomet. Chem*., in press.
(11) (a) Chen, G.; Leong, W. K. *J. Chem. Soc., Dalton Trans*. **1998**, 2489. (b) Chen, G.; Leong, W. K. *J. Organomet. Chem*. **1999**, *574*, 276. (c) Leong, W. K.; Chen, G. *J. Chem. Soc., Dalton Trans*. **2000**, 4442.

10.1021/om010039s CCC: $20.00
Publication on Web 05/01/2001

Scheme 1

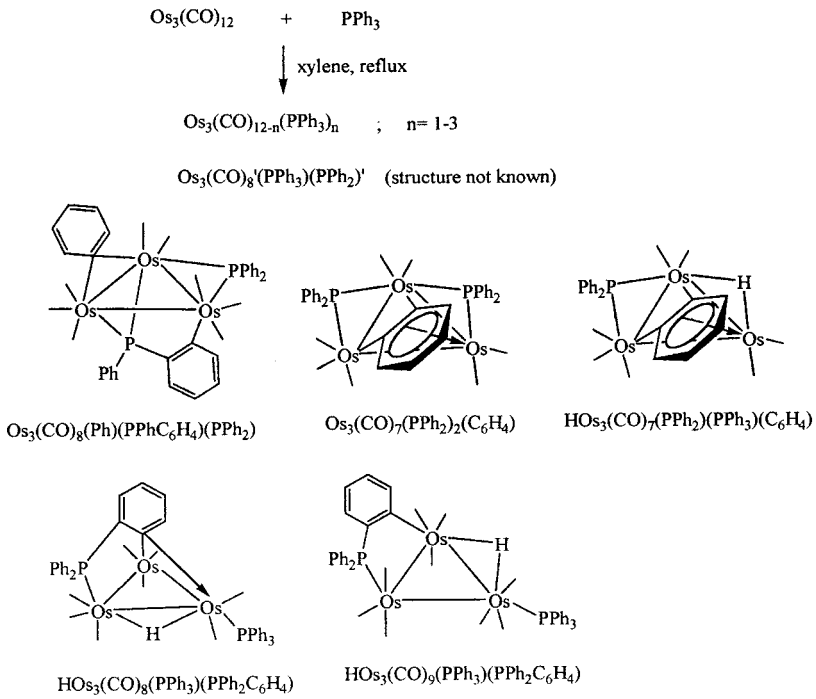

ally different complexes. In this paper, we report on our work with the monosubstituted triphenylstibine derivative $Os_3(CO)_{11}(SbPh_3)$, **1**.

Results and Discussion

When a suspension of **1** was heated under reflux in octane, the color of the solution changed from yellow to orange. When the reflux was halted after half an hour, and the mixture separated by TLC, two other major bands besides unreacted **1** were obtained. The first of these afforded $Os_3(\mu\text{-}SbPh_2)(\mu\text{-}H)(\mu_3,\eta^2\text{-}C_6H_4)(CO)_9$, **2**, as a yellow solid. Cluster **2** is closely related to the known arsenic analogues $Os_3(\mu\text{-}AsR_2)(\mu\text{-}H)(\mu_3,\eta^2\text{-}C_6H_4)(CO)_9$, products from the pyrolysis of the arsine-substituted clusters $Os_3(CO)_{11}(AsR_2Ph)$ (R = Me,[12] Ph[10]); they have similar patterns in their IR spectrum for the carbonyl stretching region. The structure of **2** has been confirmed by a single-crystal X-ray crystallogaphic study (Figure 1). The second TLC band gave a red solid, the identity of which was determined by X-ray crystallography as the novel cluster $Os_6(\mu_3\text{-}SbPh)(\mu_3,\eta^2\text{-}C_6H_4)(CO)_{20}$, **3** (Figure 2). Cluster **3** comprises two discrete Os_3 triangles that are linked via a μ_3-SbPh moiety; one of the triosmium units carries a μ_3,η^2-benzyne ligand.

The prolonged reflux of **1** in octane (5 h) gave a dark red solution and a brown precipitate. Chromatographic separation of the reaction mixture gave many products in low yields, one of which was a red crystalline material identified as the novel cluster $Os_6(\mu_4\text{-}Sb)(\mu\text{-}H)(\mu_3,\eta^2\text{-}C_6H_4)(\mu_3,\eta^4\text{-}C_{12}H_8)(CO)_{16}$, **4** (Figure 3). The structure of **4** exhibits two triosmium units that are linked via a μ_4-antimony atom. Another novel feature is the presence of a biphenylene ligand, the formation of which must involve a multistep process, including Sb−C cleavage,

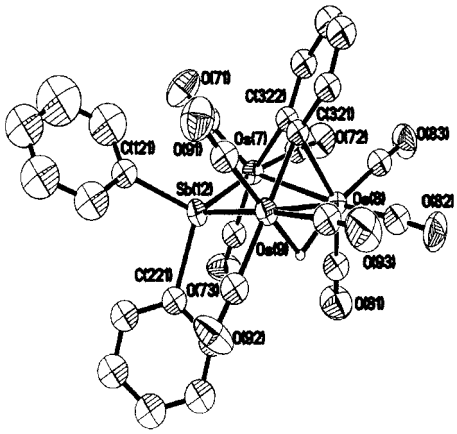

Figure 1. ORTEP diagram (organic hydrogens omitted, 50% probability thermal ellipsoids) and selected bond parameters for the ordered molecule of **2**. Os(7)−Os(8) = 2.8538(6) Å; Os(8)−Os(9) = 2.9788(6) Å; Os(7)−Sb(12) = 2.6473(9) Å; Os(9)−Sb(12) = 2.6481(9) Å; ∠Os(7)Os(8)Os(9) = 87.838(17)°; ∠ Os(7)Sb(12)Os(9) = 99.67(3)°; ∠Sb(12)Os(7)Os(8) = 84.64(2)°; ∠Sb(12)Os(9)Os(8) = 82.18(2)°.

C−C bond formation, and oxidative addition of C−H bonds. Thus in contrast to the phosphine and arsine analogues, the thermolysis of **1** in octane resulted in condensation reactions to higher nuclearity clusters.

The mechanism by which cluster expansion occurs is thought to involve formation of coordinatively unsaturated species by dissociation of ligands or cleavage of M−M bonds; these coordinatively unsaturated fragments are apparently the key intermediates that condense to give high nuclearity clusters.[13] We believe that the initial decarbonylation compound, **2**, obtained from Sb−C and Os−Os bond cleavages and ortho C−H bond activation from **1**, played an important role in the

(12) Deeming, A. J.; Rothwell, I. P.; Hursthouse, M. B.; Backer-Dirks, J. D. J. *J. Chem. Soc., Dalton Trans.* **1981**, 1879.

(13) (a) Johnson, B. F. G.; Lewis, J. *Adv. Inorg. Chem. Radiochem.* **1981**, *24*, 225. (b) Vargas, M. D.; Nicholls, J. N. *Adv. Inorg. Chem. Radiochem.* **1986**, *30*, 123.

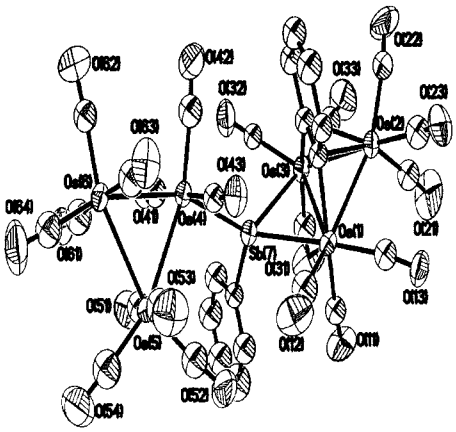

Figure 2. ORTEP diagram (organic hydrogens omitted, 50% probability thermal ellipsoids) for molecule 1 of **3**.

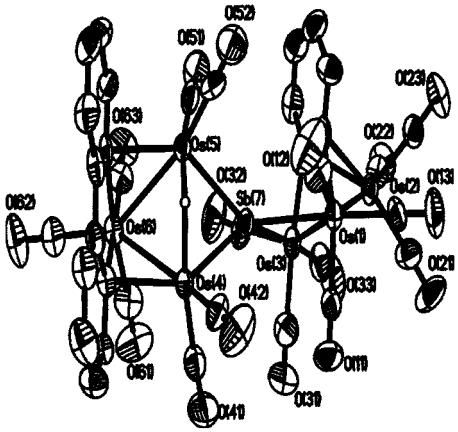

Figure 3. ORTEP diagram (organic hydrogens omitted, 50% probability thermal ellipsoids) for **4**.

formation of **3** and **4**. Cluster **3** may conceivably be formed by the attack of an "$Os_3(CO)_{11}$" moiety on **2**. It has been suggested that in the reactions of $Os_3(CO)_{11}(PMe_2Ph)$ a CO group initially dissociates, whereas in the $AsMe_2Ph$ analogue, the arsine ligand, which is more weakly bound than the phosphine, could dissociate in competition with CO.[14] We therefore conjectured that dissociation of $SbPh_3$ from **1** may have occurred during the reaction to afford the "$Os_3(CO)_{11}$" moiety. We initially attempted to verify this by refluxing **2** with $Os_3(CO)_{11}(NCCH_3)$ or $Os_3(CO)_{12}$ in octane, but no **3** was observed. We thought that perhaps this may be due to the poor solubility of $Os_3(CO)_{11}(NCCH_3)$ and $Os_3(CO)_{12}$ in octane. We then tried reacting **2** with 1 equiv of **1**; this gave cluster **3** in higher yield than the direct thermolysis of **1** (40% vs 10%); the reaction was also more facile (shorter reaction time and lower temperature). Also consistent with this, we have found that thermolysis of **1** under a CO atmosphere gave mainly $Os_3(CO)_{12}$, pointing to dissociation of the $SbPh_3$ ligand.

That **2** was not observed in the reaction mixture on prolonged reflux indicated that **2** was likely also the precursor to **4**, possibly via **3** as an intermediate; the latter possibility was suggested by the structural similarities between **3** and **4**. We conjectured that **3** may decarbonylate and undergo an Sb−C bond cleavage and a C−C coupling to afford **4**. We thus heated **3** in the

(14) Deeming, A. J.; Kimber, R. E.; Underhill, M. *J. Chem., Soc., Dalton Trans.* **1973**, 2589.

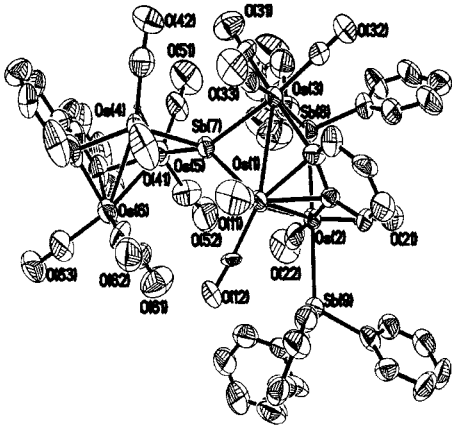

Figure 4. ORTEP diagram (organic hydrogens omitted, 50% probability thermal ellipsoids) for **8**.

presence of benzene; the added benzene could conceivably act as a source of phenyl for the formation of the biphenylene moiety. As it turned out, there was no change in the IR spectrum of the reaction mixture even after 5 h of heating. In contrast, in the absence of benzene, refluxing **3** in octane led to a rapid change in the color of the solution from pink-red to dark red; TLC separation afforded several bands but no **4**. These reactions demonstrated that **3** probably decomposed via loss of benzene and that **4** was not derived from **2** via **3** but via some other intermediate.

In an attempt to control the thermal decomposition, we also carried out a thermolysis of **1** in hexane at 115 °C in a Carius tube. After 20 h of heating, an orange-red solution and a brown precipitate were obtained, from which five clusters (besides unreacted **1**) were isolated (Scheme 2).

The new clusters $Os_6(\mu_4\text{-Sb})(\mu\text{-SbPh}_2)(\mu\text{-H})_2(\mu_3,\eta^2\text{-}C_6H_4)(\mu_3,\eta^4\text{-}C_{12}H_8)(C_6H_5)(CO)_{15}$, **5**, $Os_6(\mu_4\text{-Sb})(\mu\text{-SbPh}_2)(\mu\text{-H})(\mu_3,\eta^2\text{-}C_6H_4)2(CO)_{16}$, **6**, and $Os_6(\mu_4\text{-Sb})(\mu\text{-SbPh}_2)(\mu\text{-H})(\mu_3,\eta^2\text{-}C_6H_4)(\mu_3,\eta^6\text{-}C_6H_4)(C_6H_5)(CO)_{15}$, **7**, were characterized by IR and NMR spectroscopy, elemental analyses, and single-crystal X-ray crystallographic studies. Despite numerous attempts at growing a suitable crystal of **5**, however, we invariably ended up with extremely thin plates, which afforded data sets that were of a quality that was sufficient to establish the heavy atom positions, but not enough to provide reliable data on the light atoms. We thus attempted to obtain a substitution derivative that would afford good diffraction quality crystals, which would then allow corroboration of the proposed structure of **5**. We were fortunate in that the reaction of **5** at room temperature with $SbPh_3$ proceeded smoothly to give a red solution, from which one product was obtained after TLC separation. The molecular structure of this compound has been determined by a single-crystal X-ray crystallographic study as $Os_6(\mu_4\text{-Sb})(\mu\text{-H})_2(\mu\text{-SbPh}_2)(\mu_3,\eta^2\text{-}C_6H_4)(\mu_3,\eta^4\text{-}C_{12}H_8)(CO)_{14}(SbPh_3)$, **8** (Figure 4).

The structures of **5**, **6**, and **7** are closely related (Figures 5 and 6, Scheme 2). All three clusters have similar metal skeletons; the main differences lie in their ligand sets. The route for the formation of cluster **6** was suggested by the structure of the compound itself; **6** may be considered as being derived from the condensation of two molecules of **2**. Indeed, thermolysis of **2** did afford a high yield of cluster **6**.

Scheme 2

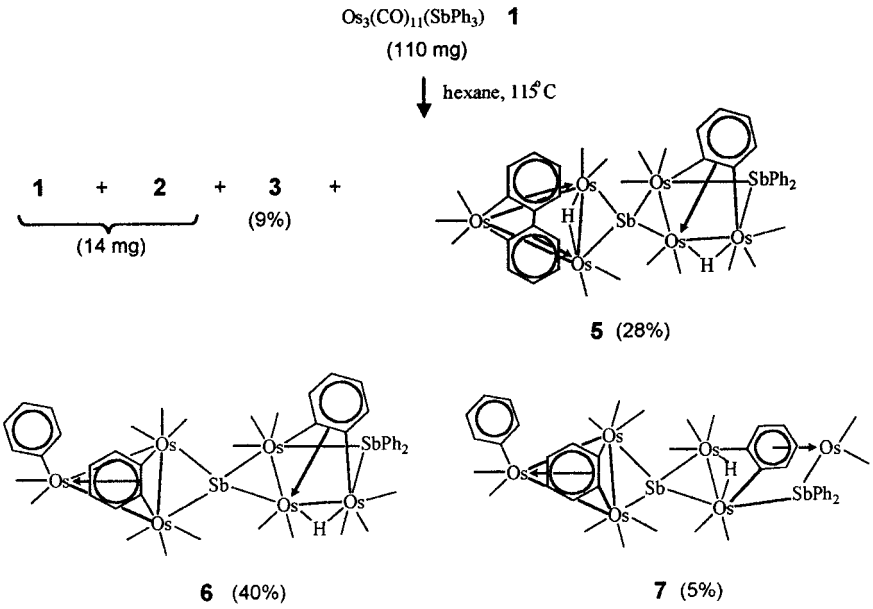

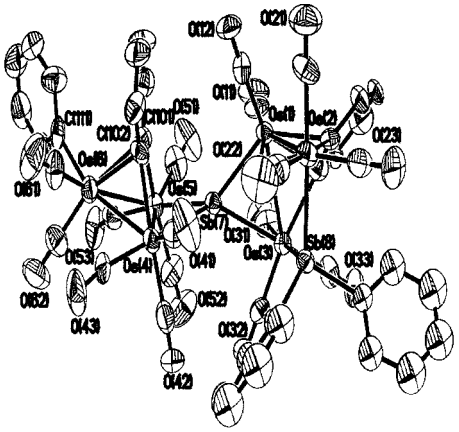

Figure 5. ORTEP diagram (organic hydrogens omitted, 50% probability thermal ellipsoids) for **6**.

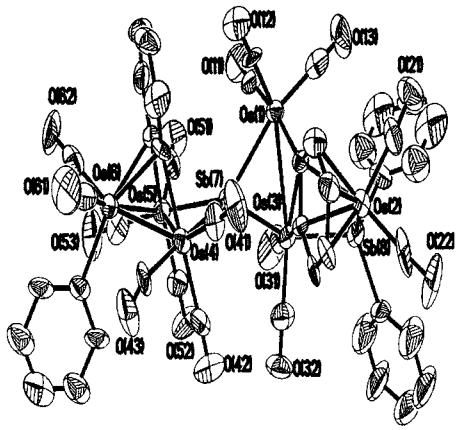

Figure 6. ORTEP diagram (organic hydrogens omitted, 50% probability thermal ellipsoids for **7**.

The similarity of the structures of **5**, **6**, and **7** suggested that they may be related mechanistically. For example, **5** may be formed from **6** by an intracluster oxidative addition of the benzyne into the β C−H bond of the terminal phenyl ligand. UV irradiation (15 W, 360 nm) of a CH_2C_{l2} solution of **6** was monitored by IR spectroscopy and indicated that **6** was photochemically quite robust. Heating a solution of **6** in hexane at 110 °C for 2 h gave **5** (70%) and **7** (10%) as the major products, thus indicating that both **5** and **7** were derived from **6** by further competitive decomposition (Scheme 3). The formation of **5** from **6** should be a multistep process, involving the elimination and migration of CO ligands, C−H and Os−C bond cleavage, and C−C bond formation, but the sequence of these processes remains unknown. Although the elimination of only one carbonyl and cleavage of an Os−Os bond in **6** could stoichiometrically lead to **7**, the yield was much lower than expected. This suggested that the $Os_3(\mu\text{-}SbPh_2)(\mu\text{-}H)(\mu_3,\eta^2\text{-}C_6H_4)(CO)_8$ subunit in **6** is more robust than its other subunit.

Crystallographic Studies

Cluster **2** has three crystallographically distinct molecules in the asymmetric unit, two of which showed disorder about the Os_3Sb core; the ordered molecule, together with its selected bond parameters, is shown in Figure 1. The $SbPh_2$ fragment forms a symmetrical bridge across the Os(7)···Os(9) edge; at 4.05 Å this is clearly nonbonding, and electron count requires that the μ_3,η^2-C_6H_4 ligand acts as a four-electron donor. The metal hydride was not located in the X-ray crystal structure; its position was calculated with the program XHYDEX[15] as bridging the longer Os(8)−Os(9) edge, in accord with general observations in triosmium cluster chemistry.

Selected bond parameters involving the heavy atoms for clusters **3**, **4**, **6**, **7**, and **8** are given in Table 1; there are two crystallographically distinct molecules in **3**. With the exception of **3**, all the other clusters are characterized by the presence of a μ_4-Sb moiety joining two triosmium units, and bridging metal hydrides. The presence of the bridging hydrides were indicated in their ^{1}H NMR spectra, and their positions were determined

(15) Orpen, A. G. *XHYDEX*: A Program for Locating Hydrides in Metal Complexes; School of Chemistry, University of Bristol: UK, 1997.

Scheme 3

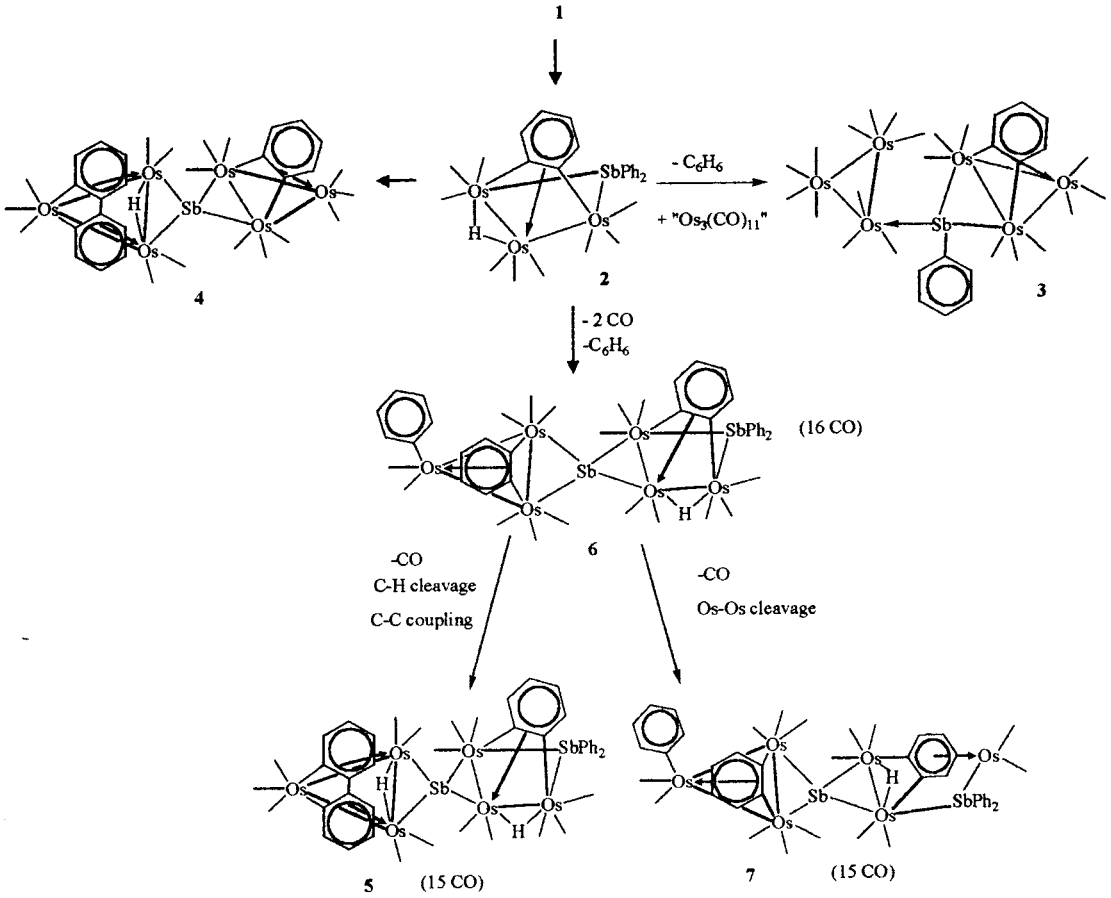

Table 1. Selected Bond Parameters for Clusters 3, 4, 6, 7, and 8

bond parameter	3	4	6	7	8
Os(1)−Os(2)	2.7939(12); 2.8024(10)	2.7778(6)	2.9113(9)		2.9547(9)
Os(1)−Os(3)	2.9095(11); 2.9101(11)	2.9368(6)	2.9422(8)	3.0165(10)	3.0037(9)
Os(2)−Os(3)	2.7739(10); 2.7659(12)	2.7907(6)			
Os(4)−Os(5)	2.9133(12); 2.9174(10)	2.9022(6)	2.8943(9)	2.8716(11)	2.9241(11)
Os(4)−Os(6)	2.8704(11); 2.8794(10)	2.8875(6)	2.8466(9)	2.7962(12)	2.8869(11)
Os(5)−Os(6)	2.8910(12); 2.8824(11)	2.8812(6)	2.8188(9)	2.8089(10)	2.8741(11)
Os(1)−Sb(7)	2.7170(14); 2.7201(15)	2.6960(8)	2.5376(11)	2.6762(15)	2.5713(12)
Os(3)−Sb(7)	2.7240(16); 2.7263(13)	2.6911(8)	2.7664(11)	2.5929(15)	2.7763(12)
Os(4)−Sb(7)	2.6327(15); 2.6344(14)	2.5504(8)	2.6306(11)	2.6583(14)	2.5589(13)
Os(5)−Sb(7)		2.5529(8)	2.6474(12)	2.6452(15)	2.5663(13)
Os(2)−Sb(8)			2.6310(11)	2.6447(15)	2.6235(13)
Os(3)−Sb(8)			2.6621(12)	2.6125(16)	2.6912(14)
Os(2)−Sb(9)					2.6695(13)
Os(1)−Sb(7)−Os(3)	64.65(4); 64.59(3)	66.07(2)	67.22(3)	69.83(4)	68.22(3)
Os(4)−Sb(7)−Os(5)		69.32(2)	66.51(3)	65.57(4)	69.57(4)
Os(2)−Sb(8)−Os(3)			101.04(4)	93.97(5)	102.13(4)

by potential energy calculations using XHYDEX, with the exception of **7**, in which the hydride was located in a low-angle difference map.

This structural feature of a spirocyclic μ_4-Sb has been observed in one instance for iron,[16] but the clusters presented here are the first examples from osmium cluster chemistry. An interesting observation here is that there is a large Os−Os bond lengthening effect of a bridging Sb: the Os−Os edges bridged by the μ_4-Sb (Os(1)−Os(3) for **3**, **4**, **6**, **7**, and **8** and Os(4)−Os(5) for **4**, **6**, **7**, and **8**) are invariably the longest of the Os−Os edges in a given triosmium unit; this effect is even greater than that of a bridging hydride,[17] as is most readily discerned in **4**, **6**, and **8**.

The Os−Sb bond lengths vary from 2.5376(11) Å in **6** to 2.7763(12) Å in **8**; in fact, the upper limit is longer than the Os(2)−Os(3) bond in **3** (2.7728(10) and 2.7657(11) Å). On the other hand, ∠Os−Sb−Os angles can vary from 64.59(3)° to 69.83(4)° over a "closed" Os−Os edge and from 93.97(5)° to 102.13(4)° over an "open" Os···Os edge. It is therefore quite apparent that the bond parameters associated with the antimony atoms vary over a wide range, indicating that antimony can accommodate a large amount of molecular distortions.

Cluster **3** comprises two discrete Os_3 triangles that are linked via a μ_3-SbPh moiety; one of the triosmium

(16) Rheingold, A. L.; Geib, S. J.; Shieh, M.; Whitmire, K. H. *Inorg. Chem.* **1987**, *26*, 463.

(17) (a) Leong, W. K. M.Sc. Thesis, National University of Singapore, 1992. (b) Churchill, M. R.; DeBoer, B. G.; Rotella, F. J. *Inorg. Chem.* **1976**, *15*, 1843. (c) Bau, R.; Teller, R. G.; Kirtley, S. W.; Koetzle, T. F. *Acc. Chem. Res.* **1979**, *12*, 176.

Scheme 4

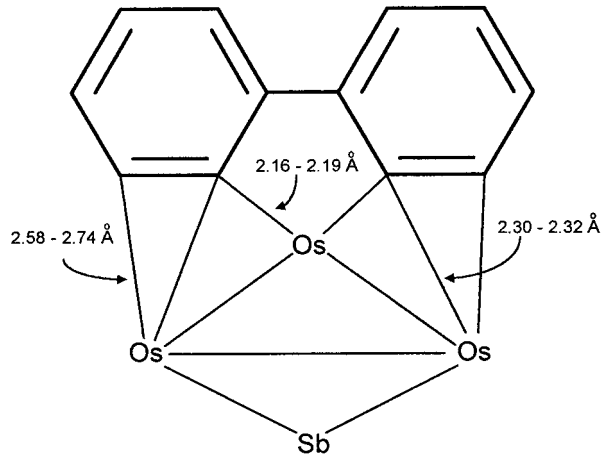

units carries a μ_3,η^2-benzyne ligand, while the other is an "$Os_3(CO)_{11}$" unit. The Os−Os edge on this "$Os_3(CO)_{11}$" unit that is cis to the Os−Sb bond (Os(1)−Os(2) and Os(4)−Os(5)) is elongated with respect to the other Os−Os edges (2.9137(11) and 2.9175(9) Å, respectively, for the two crystallographically distinct molecules, compared to 2.8708(11)−2.8912(11) Å for the other edges); this is consistent with the observation that the substitution of a CO group by a σ-donating ligand at an equatorial position in a triosmium unit usually results in the lengthening of the M−M bond cis to it.[18] In other words, the $(\mu$-SbPh$)Os_3(CO)_9(\mu_3,\eta^2$-$C_6H_4)$ group may be regarded as a very bulky stibine toward the "$Os_3(CO)_{11}$" unit.

A novel feature in **4**, **5**, and **8** is the presence of a biphenylene ligand. One of the osmium atoms (Os(6)) lies in the plane of the biphenylene ligand, and the ligand is tilted toward the other two osmiums; the dihedral angles between the Os(4)Os(5)Os(6) and biphenylene planes are 66.2° and 66.4° for **4** and **8**, respectively. Thus the bonding situation can be described as comprising two σ interactions to the unique osmium atom and an η^2 interaction each to the two osmium atoms that are bridged by the antimony atom; the Os···C distances involved in such a bonding situation range from about 2.16 Å to 2.74 Å (Scheme 4), while the other Os···C distances are all > 3.0 Å. This is a novel bonding mode for biphenyl; a closely related example is that found in the dinuclear clusters $M_2(CO)_6(\mu,\eta^4$-$C_{12}H_8)$ (M = Fe, Ru, Os), in which the biphenylene exhibits two σ interactions to one metal atom and an η^4 interaction to the other.[19] Other bonding modes observed involve only one of the aromatic rings, either via an η^2 interaction (to a triosmium cluster)[19] or an η^6 interaction (in ruthenium clusters).[20] In assigning electron count, it has been found convenient to consider the two Os_3 units in the $Os_3(\mu_4$-Sb$)Os_3$ clusters separately. For instance, in **4**, the μ_4-Sb may be regarded as contributing two electrons to the $Os_3(\mu$-SbPh$)(\mu$-H$)(CO)_8(\mu_3,\eta^2$-$C_6H_4)$ fragment; this satisfies the EAN rule for the fragment. The μ_4-Sb can then be considered to contribute three electrons to the Os_3 fragment carrying the biphenylene ligand, and hence the latter should be regarded as a six-electron donor in order to satisfy the EAN rule.

Cluster **7** also possesses an interesting structural feature; there is a C_6H_4 unit that appears to be σ-bonded to two osmium atoms (Os(1) and Os(3)) and η^6-coordinated to Os(2). This would imply that the C_6H_4 unit is acting as an eight-electron donor ligand; consistent with this is the presence of only one Os−Os bond, as required by the electron count. There is no analogue to **7** known in osmium cluster chemistry, although the feature of a μ_3,η^6-C_6H_4 unit has been observed in some triruthenium−chromium clusters that were obtained from the reaction of $Ru_3(CO)_{12}$ with some η^6-C_6H_5Cr-containing precursor like $P[C_6H_5Cr(CO_3)]_2Ph$ or $P[C_6H_5$-$Cr(CO_3)]_2Bu^t$ and from the pyrolysis of $Ru_3(CO)_{11}$-$[AsMe_2C_6H_5Cr(CO)_3]$;[21] all these have η^6-coordination to a Cr atom.

Conclusion

In this paper, we have reported that the thermolysis of **1** at ∼120 °C gave initially the trinuclear cluster **2**. Over a longer reaction time, and depending on the control of CO loss, higher nuclearity clusters **3**−**7** were formed in varying amounts. All of these higher nuclearity clusters represent new structural types in osmium−antimony cluster chemistry and are the first examples of higher nuclearity clusters of osmium and antimony containing a μ_4-Sb moiety. The structural details show that there is capacity for a wide variation in bond parameters involving antimony. The relationship among these clusters is depicted in Scheme 3. Formation of the higher nuclearity clusters found necessarily involves Os−Sb and C−C bond formation and Sb−C and C−H bond cleavage. Thus compared to osmium−phosphorus or −arsenic clusters, osmium−antimony clusters exhibit a greater tendency to form higher nuclearity clusters via condensation at an antimony atom.

Experimental Section

General Experimental Procedures. Manipulations were carried out using standard Schlenk techniques under a nitrogen atmosphere.[22] Cluster **1** was prepared from the reaction of $SbPh_3$ (commercial source) and $Os_3(CO)_{11}(CH_3$-$CN)$.[23] NMR spectra were recorded on a Bruker ACF-300FT-NMR spectrometer as $CDCl_3$ solutions. Microanalyses were carried out by the microanalytical laboratory at the National University of Singapore. The presence of solvent molecules in samples used for elemental analyses or X-ray crystallographic studies was confirmed by ^{1}H NMR spectroscopy.

Thermolysis of 1 in Refluxing Octane. A sample of **1** (110 mg, 0.089 mmol) in octane (20 mL) was refluxed until the color of the solution changed from bright yellow to orange

(18) (a) Beringhelli, T.; D'Alfonso, G.; Minojia, A. P. *Organometallics* **1991**, *10*, 394. (b) Andreu, P. L.; Cabeza, J. A.; Pellinghelli, M. A.; Riera, V.; Tiripicchio, A. *Inorg. Chem.* **1991**, *30*, 4611. (c) Farrugia, L. J.; Rae, S. E.; *Organometallics* **1991**, *10*, 3919. (d) Bruce, M. I.; Liddell, M. J.; Hughes, C. A.; Skelton, B. W.; White, A. H. *J. Organomet. Chem.* **1988**, *347*, 157. (e) Sappa, E.; Tiripicchio, A.; Carty, A. J.; Toogood, G. E. *Prog. Inorg. Chem.* **1987**, *35*, 437, and references therein.

(19) Yeh, W.-Y.; Hsu, S. C. N.; Peng, S.-M.; Lee, G.-H. *Organometallics* **1998**, *17*, 2477.

(20) Johnson, B. F. G.; Shephard, D. S.; Braga, D.; Grepioni, F.; Parsons, S. *J. Chem., Soc., Dalton Trans.* **1997**, 3563.

(21) (a) Cullen, W. R.; Rettig, S. T.; Zhang, H. *Organometallics* **1991**, *10*, 2965. (b) Cullen, W. R.; Rettig, S. T.; Zhang, H. *Organometallics* **1992**, *11*, 1000. (c) Cullen, W. R.; Rettig, S. T.; Zhang, H. *Organometallics* **1993**, *12*, 1964.

(22) Shriver, D. F.; Drzedzon, M. A. *The Manipulation of Air-Sensitive Compounds*, 2nd ed.; Wiley: New York, 1986.

(23) Nicholls, J. N.; Vargas, M. D. *Inorg. Synth.* **1989**, *28*, 232.

Published on May 1, 2001 on http://pubs.acs.org | doi: 10.1021/om010039s

Table 2. Crystal Data for 2, 3, 4, 6, 7, and 8

	2	3	4	6	7	8
formula	$C_{27}H_{15}O_9Os_3Sb$	$2C_{32}H_9O_{20}Os_6Sb$	$C_{34}H_{13}O_{16}Os_6Sb\cdot 1/2$toluene	$C_{46}H_{24}O_{16}Os_6Sb_2\cdot 2CH_2Br_2$	$C_{45}H_{24}O_{15}Os_6Sb_2$	$C_{62}H_{39}O_{14}Os6Sb_3$
fw	1175.74	3952.68	1986.46	2565.04	2189.34	2514.38
cryst syst	monoclinic	triclinic	monoclinic	triclinic	triclinic	triclinic
space group	*P*21/*c*	$P\bar{1}$	*P*21/*c*	$P\bar{1}$	$P\bar{1}$	$P\bar{1}$
a, Å	9.6411(1)	12.1113(2)	9.5383(1)	11.4224(2)	9.4642(2)	12.1127(1)21.
b, Å	35.7932(5)	16.0140(1)	17.9231(2)	15.0997(1)	16.3515(2)	14.8188(2)
c, Å	25.7982(1)	23.6010(2)	25.5182(1)	18.7657(1)	17.8223(3)	21.5848(1)
α, deg	90	106.722(1)	90	111.664(1)	83.222(1)	82.299(1)
β, deg	92.84(1)	92.173(1)	98.60(1)	92.948(1)	74.722(1)	76.949(1)
γ, deg	90	106.738(1)	90	102.589(1)	75.868(1)	70.891(1)
volume, Å^3	3558.73(6)	4161.55(8)	4313.38(7)	2904.47(6)	2575.82(8)	3558.73(6)
no. of reflns for unit cell	8192	8192	7814	8192	5302	6499
Z	12	2	4	2	2	2
ρ_c, g cm-3	2.635	3.154	3.059	2.933	2.823	2.346
μ(Mo Kα), mm^{-1}	13.770	18.959	18.286	16.797	15.829	11.839
F(000)	6336	3472	3508	2284	1944	2264
cryst size, (mm)	0.26 × 0.18 × 0.09	0.22 × 0.10 × 0.01	0.22 × 0.22 × 0.10	0.30 × 0.20 × 0.14	0.14 × 0.07 × 0.02	0.43 × 0.28 × 0.06
θ range, deg	2.11 to 29.41	2.00 to 29.25	2.16 to 29.38	2.04 to 29.62	2.29 to 29.53	1.70 to 29.22
no. of reflns colld	62 778	31 296	32 479	22 096	19 833	25 649
no. of ind reflns	22 147 (R_{int}=0.0550)	19 664 (R_{int}=0.0674)	10 861 (R_{int}=0.0688)	13 867 (R_{int}=0.0513)	13 299 (R_{int}=0.0720)	16 148 (R_{int}=0.0707)
transmn range	0.264323−0.129578	0.280083−0.102030	0.162226−0.074351	0.13869−0.025066	0.595711−0.309925	0.154251−0.063901
no. of data/restraints/params	22 147/4/588	19 664/0/743	10 861/0/531	13 867/15/614	12 401/0/541	16 148/6/742
goodness-of-fit on F^2	1.189	0.927	0.987	0.981	0.919	0.936
final *R* indices [$I>2\sigma(I)$]	R1 = 0.0599 R2 = 0.0991	R1 = 0.0595 wR2 = 0.1221	R1 = 0.0450 wR2 = 0.0982	R1 = 0.0571 wR2 = 0.1342	R1 = 0.0636 wR2 = 0.1147	R1 = 0.0687 wR2 = 0.1689
R indices (all data)	R1 = 0.0885 wR2 = 0.1074	R1 = 0.1462 wR2 = 0.1491	R1 = 0.0758 wR2 = 0.1088	R1 = 0.1110 wR2 = 0.1606	R1 = 0.1690 wR2 = 0.1502	R1 = 0.1288 wR2 = 0.2072
largest diff peak and hole, e Å^{-3}	1.556 and −1.651	2.223 and −3.270	2.678 and −2.251	2.358 and −2.403	2.690 and −2.334	2.660 and −3.988

(30 min). Removal of the solvent followed by TLC separation using hexane as eluant gave three bands.

Band 1 gave $Os_3(\mu\text{-H})(\mu\text{-SbPh}_2)(\mu_3,\eta^2\text{-C}_6H_4)(CO)_9$, **2** (45 mg, 43%): IR (hexane) ν(CO) 2091w, 2071vs, 2043vs, 2018m, 2004m, 1988w, 1971w cm^{-1}; ^{1}H NMR δ −17.81 (s, OsHOs). Anal. Cald for $C_{27}H_{15}O_9Os_3Sb.1/2C_6H_{14}$: C, 29.55; H, 1.80. Found: C, 29.94; H, 1.50.

Band 2 gave unreacted **1** (40 mg, 36%).

Band 3 gave red crystals of $Os_6(\mu_3\text{-SbPh})(\mu_3,\eta^2\text{-C}_6H_4)(CO)_{20}$, **3** (9 mg, 10%): IR (CH_2Cl_2) ν(CO) 2108w, 2094vs, 2058vs, 2028vs, 1987w, 1973w cm^{-1}. Anal. Calcd for $C_{32}H_9O_{20}Os_6Sb$: C, 19.43; H, 0.46. Found: C, 19.69; H, 0.25.

Prolonged heating of **1** (∼5 h) gave a dark red solution and a brown precipitate. TLC separation of the reaction mixture using CH_2Cl_2/hexane (30:70, v/v) as eluant gave $Os_6(\mu_4\text{-Sb})(\mu\text{-H})(\mu_3,\eta^2\text{-C}_6H_4)(\mu_3,\eta^4\text{-C}_{12}H_8)(CO)_{16}$, **4**, as the major product (17 mg, 20%): IR (hexane) ν(CO) 2098m, 2067m, 2057s, 2025s, 2008m, 2000m, 1986w,1948w cm^{-1}; ^{1}H NMR δ −13.66 (s, OsHOs). Anal. Calcd for $C_{34}H_{13}O_{16}Os_6Sb$: C, 21.03; H, 0.67. Found: C, 21.15; H, 0.93. No **2** or **3** was observed among the products.

Thermolysis of 1 in a Carius Tube. A sample of **1** (110 mg, 0.089 mmol) was placed in a Carius tube with hexane (15 mL), and the reaction mixture degassed by three freeze−pump−thaw cycles. The suspension was then heated at 115 °C for 17 h, upon which the color of the solution changed from yellow to red. TLC separation of the mixture with CH_2Cl_2/hexane (30:70, v/v) as eluant gave the following bands.

Band 1 gave a mixture containing both **1** and **2** (14 mg). Band 2 gave **3** (8 mg, 9%).

Band 3 gave red crystals of $Os_6(\mu_4\text{-Sb})(\mu\text{-H})_2(\mu\text{-SbPh}_2)(\mu_3,\eta^2\text{-C}_6H_4)(\mu_3,\eta^4\text{-C}_{12}H_8)(CO)_{15}$, **5** (27 mg, 28%): IR (CH_2Cl_2) ν(CO) 2096m, 2080s, 2057s, 2027vs, 1998s, 1942m cm^{-1}; ^{1}H NMR δ −12.97 (s, OsHOs), −13.83 (s, OsHOs). Anal. Calcd for $C_{45}H_{24}O_{15}Os_6Sb_2$: C, 24.67; H, 1.10. Found: C, 24.88; H, 0.66.

Band 3 gave red crystals of $Os_6(\mu_4\text{-Sb})(\mu\text{-H})_2(\mu\text{-SbPh}_2)(\mu_3,\eta^2\text{-C}_6H_4)(\mu_3,\eta^4\text{-C}_{12}H_8)(CO)^{15}$, **5** (27 mg, 28%): IR (CH_2C_{l2}) ν(CO) 2096m, 2080s, 2057s, 2027vs, 1998s, 1942m cm^{-1}; ^{1}H NMR δ −12.97 (s, OsHOs), −13.83 (s, OsHOs). Anal. Calcd for $C_{45}H_{24}O_{15}Os_6Sb_2$: C, 24.67; H, 1.10. Found: C, 24.88; H, 0.66.

Band 4 gave red crystals of $Os_6(\mu_4\text{-Sb})(\mu\text{-H})(C_6H_5)(\mu\text{-SbPh}_2)(\mu_3,\eta^2\text{-C}_6H_4)_2(CO)_{16}$, **6** (37 mg, 40%): IR (hexane) ν(CO) 2098w, 2086vs, 2060m, 2042vs, 2031s, 2016s, 1991w, 1962m cm^{-1}; ^{1}H NMR δ −14.63 (s, OsHOs). Anal. Calcd for $C_{46}H_{24}O_{16}Os_6Sb_2$: C, 24.90; H, 1.08. Found: C, 25.30; H, 1.44.

Band 5 gave orange crystals of $Os_6(\mu_4\text{-Sb})(\mu\text{-H})(C_6H_5)(\mu\text{-SbPh}_2)(\mu_3,\eta_2\text{-C}_6H_4))(\mu_3,\eta^6\text{-C}_6H_4)(CO)_{15}$, **7** (5 mg, 5%): IR ($CH_2Cl_2$) ν(CO) 2086m, 2053s, 2032s, 2008s, 1988m, 1954m cm^{-1}; ^{1}H NMR δ −11.93 (s, OsHOs). Anal. Calcd for $C_{45}H_{24}O_{15}Os_6Sb_2$: C, 24.67; H, 1.10. Found: C, 25.01; H, 0.86.

Thermolysis of 2. A sample of **2** (30 mg, 0.026 mmol) was placed in a Carius tube with hexane (10 mL), and the reaction mixture degassed by three freeze−pump−thaw cycles. The suspension was then heated at 115 °C for 15 h, upon which the color of the solution changed from yellow to orange. TLC separation of the mixture using CH_2Cl_2/hexane (30:70, v/v) as eluant gave **6** as the major compound, which was identified by its IR spectroscopic characteristics (20 mg, 73%).

Thermolysis of 6. A sample of **6** (30 mg, 0.014 mmol) was placed in a Carius tube with hexane (10 mL), and the reaction mixture degassed by three freeze−pump−thaw cycles. The suspension was then heated at 110 °C for 3 h. TLC separation of the mixture using dichloromethane/hexane (1:1, v/v) gave **5** (21 mg, 70%) and **7** (3 mg, 10%).

Reaction of 5 with $SbPh_3$. To a solution of cluster **5** (32 mg, 0.015 mmol) in dichloromethane (15 mL) was added $SbPh_3$ (10 mg, 0.026 mmol). The solution was then stirred for 20 h. Removal of the solvent followed by TLC separation using CH_2Cl_2/hexane (40:60, v/v) as eluant gave two bands.

Band 1 gave unreacted **5** (3 mg).

Band 2 gave $Os_6(\mu_4\text{-Sb})(\mu\text{-H})_2(\mu\text{-SbPh}_2)(\mu_3,\eta^2\text{-C}_6H_4)(\mu_3,\eta^4\text{-C}_{12}H_8)(CO)_{14}(SbPh_3)$, **8** (28 mg, 76%): IR (CH_2C_{l2}) ν(CO) 2080m, 2056s, 2023vs, 1995s, 1969w, 1940m cm^{-1}; ^{1}H NMR δ −12.65 (s, OsHOs), −13.26 (s, OsHOs). Anal. Calcd for $C_{62}H_{39}O_{14}Os_6Sb_3\cdot 1/4C_6H_{14}$: C, 30.07; H, 1.69. Found: C, 30.04; H, 1.88.

Reaction of 1 with CO. A suspension of **1** (104 mg, 0.084 mmol) in hexane (15 mL) was pressurized with CO (10 atm) and heated at 125 °C for 20 h. A yellow precipitate was obtained, which was confirmed by IR spectroscopy to be $Os_3(CO)_{12}$. TLC separation of the reaction mixture with CH_2Cl_2/hexane (10:90, v/v) as eluant gave $Os_3(CO)_{12}$ as the major compound (total yield = 69 mg, 90%).

Reaction of 1 and 2 in Octane. Clusters **1** (50 mg, 0.041 mmol) and **2** (47 mg, 0.040 mmol) were dissolved in octane (10 mL), degassed by three freeze−pump−thaw cycles, and heated at 105 °C for 1 h. The color of the solution changed from yellow to orange. TLC separation of the reaction mixture using CH_2C_{l2}/hexane (10:90,v/v) gave unconsumed reactants (60 mg) and **3** (32 mg, 40%).

X-ray Crystallographic Studies. Diffraction-quality crystals were grown by slow cooling of solutions of the compounds in the appropriate solvent, and the crystals selected were mounted on quartz fibers or in glass capillaries. Crystal data were collected on a Siemens SMART diffractometer, equipped with a CCD detector, using Mo Kα radition (λ = 0.71073 Å) at 293 K. The data were corrected for absorption effects with SADABS.[24] Structural solution and refinement were carried out with the SHELXTL suite of programs.[25] The structure was solved by a combination of direct methods, followed by difference maps. The phenyl hydrogens and metal hydrides not located by difference maps were placed in calculated positions with the program XHYDEX.[15] All non-hydrogen atoms were given anisotropic displacement parameters in the final refinement. Refinements were on $\sum[w(F_o^2 - F_c^2)^2]$. Crystal data are tabulated in Table 2.

Acknowledgment. This work was supported by the National University of Singapore (Research Grant No. RP 982751), and one of us (G.C.) thanks the University for a Research Scholarship.

Supporting Information Available: Experimental and refinement details for the crystallographic studies, tables of crystal data and structure refinement, atomic coordinates, isotropic and anisotropic thermal parameters, complete bond parameters, and hydrogen coordinates. Crystallographic data in CIF format. This material is available free of charge via the Internet at http://pubs.acs.org.

OM010039S

(24) Sheldrick, G. M. *SADABS*, University of Göttingen, 1996.
(25) *SHELXTL*, version 5.03; Siemens Energy and Automation Inc.: Madison, WI, 1995.